UC-403

LBL-24564
Preprint

Lawrence Berkeley Laboratory
UNIVERSITY OF CALIFORNIA

EARTH SCIENCES DIVISION

Submitted to Water Resources Research

On Thermohydrological Conditions near High-level Nuclear Wastes Emplaced in Partially Saturated Fractured Tuff

Part 2. Effective Continuum Approximation

K. Pruess, J.S.Y. Wang, and Y.W. Tsang

October 1989

For Reference

Not to be taken from this room

LBL-24564 Copy 1
Bldg. 50 Library.

Prepared for the U.S. Department of Energy under Contract Number DE-AC03-76SF00098.

DISCLAIMER

This document was prepared as an account of work sponsored by the United States Government. While this document is believed to contain correct information, neither the United States Government nor any agency thereof, nor the Regents of the University of California, nor any of their employees, makes any warranty, express or implied, or assumes any legal responsibility for the accuracy, completeness, or usefulness of any information, apparatus, product, or process disclosed, or represents that its use would not infringe privately owned rights. Reference herein to any specific commercial product, process, or service by its trade name, trademark, manufacturer, or otherwise, does not necessarily constitute or imply its endorsement, recommendation, or favoring by the United States Government or any agency thereof, or the Regents of the University of California. The views and opinions of authors expressed herein do not necessarily state or reflect those of the United States Government or any agency thereof or the Regents of the University of California.

LBL-24564

On Thermohydrological Conditions near High-level Nuclear Wastes Emplaced in Partially Saturated Fractured Tuff

Part 2. Effective Continuum Approximation

K. Pruess, J. S. Y. Wang, and Y. W. Tsang

Earth Sciences Division
Lawrence Berkeley Laboratory
1 Cyclotron Road
Berkeley, California 94720

October 1989

This work was supported by the Yucca Mountain Project, Sandia National Laboratories, and by the U.S. Department of Energy under Contract No. DE-AC03-76SF00098.

LBL-24564

SAND 86-7016J

On Thermohydrologic Conditions near High-level Nuclear Wastes Emplaced in Partially Saturated Fractured Tuff

Part 2. Effective Continuum Approximation

K. Pruess, J.S.Y. Wang, and Y.W. Tsang

Earth Sciences Division, Lawrence Berkeley Laboratory
University of California, Berkeley, California 94720

Abstract

This paper presents an effective continuum approximation for modeling of fluid and heat flow in fractured porous media. The approximation is based on the thermohydrologic behavior observed in detailed simulations with explicit consideration of fracture effects (see the companion paper; Part 1, this issue). The crucial concept in the development of an effective continuum approximation is the notion of local thermodynamic equilibrium between rock matrix and fractures. Where applicable it provides a substantial simplification of the description of fluid and heat flow in fractured porous media. We derive formulas for effective continuum characteristic curves (relative permeabilities and capillary pressures) in terms of the properties of fracture and matrix continua, respectively. Numerical simulations demonstrate that under favorable conditions the effective continuum approximation closely matches predictions obtained from an explicit modeling of fracture effects. It is also demonstrated that the approximation breaks down under unfavorable conditions (very tight rock matrix). A simple criterion for the applicability of an effective continuum approximation is derived from consideration of diffusive processes. A quantitative evaluation shows the criterion to be consistent with results of our numerical simulations.

1. Introduction.

This is the second of a series of two papers dealing with the thermal and hydrologic conditions following emplacement of high-level nuclear waste packages in a partially saturated formation with both fracture and matrix porosity and permeability. In the companion paper (Part 1, this issue) we presented numerical simulations of the complex fluid flow, heat transfer, and phase transformation processes induced by a strong heat source in an unsaturated fractured-porous medium. Our aim in those simulations was to obtain detailed insight into the thermohydrologic behavior on the scale of individual fractures and matrix blocks. However, an approach in which detail on a millimeter and sub-millimeter scale is resolved is clearly not suitable for describing the behavior of flow systems on a large scale (of the order of 1 km) or for extended periods of time (10^2–10^4yr).

The "explicit discretization" approach followed in the companion paper is straightforward conceptually, and it is well suited for fundamental studies of idealized systems, but it is not practical for most "real" problems, where the amount of geometric detail and complexity would be far beyond the capacity of digital computers. Even if computationally feasible, a detailed explicit treatment of all fractures would hardly seem desirable in practice, except perhaps for systems with extremely sparse fracturing. Available field data on fracture distributions are typically rather incomplete. Moreover, in modeling thermohydrologic conditions one is usually interested in predicting averages over some macroscopic scale, and too much detail on the level of individual fractures would be redundant. It is the purpose of the present paper to introduce an approximation for modeling of fluid and heat flow in fractured-porous media which, when applicable, can provide a highly simplified yet accurate description. We seek to develop an approach which will be useful for describing multi-phase fluid and heat flow in large flow regions containing ubiquitous well-connected fractures.

A powerful approach to modeling of flow in fractured media is the double-porosity method, originally developed by Russian hydrologists (Barenblatt et al., 1960), and introduced into the petroleum literature by Warren and Root (1963). In this method, a

fractured porous medium is partitioned into (1) a primary porosity, which consists of small pores in the rock matrix, e.g., intergranular vugs or vesicles, and (2) a secondary porosity, consisting of fractures and joints. Each of the two porosities is treated as a continuum, whose properties can be characterized by means of the customary porous medium properties, i.e., permeability, porosity, and compressibility. Flow within each continuum is assumed to be porous flow, governed by Darcy's law. The global flow in the medium occurs only through the fracture continuum, while fractures and rock may interact locally by means of "interporosity" flow. In the classical double-porosity work, a quasi-steady approximation was made for interporosity flow, which is usually satisfactory for problems involving isothermal single-phase flow (Moench, 1983). However, in problems involving multi-phase fluids with large and varying compressibility, and coupled fluid and heat flow, the period of transient flow between matrix and fractures can be very long. For this type of problem, the double-porosity method was extended to a method of multiple interacting continua (MINC) by Pruess and Narasimhan (1982, 1985). The MINC-method treats interporosity flow in a fully transient way, using numerical methods.

The assumption that global flow occurs only through the network of well-connected fractures breaks down for multi-phase systems with strong capillary effects. Depending on overall phase composition, the wetting phase(s) will preferentially occupy the small pores in the rock matrix, while the non-wetting phase(s) will tend to reside in the largest voids, i.e., in the fractures (Wang and Narasimhan, 1985). If the phases tend to be highly segregated between primary and secondary porosity, then global flow of the wetting phase will take place through the primary porosity, crossing fractures at asperity contacts. Flow systems with two kinds of global flow have sometimes been referred to as "dual-permeability" reservoirs (Miller and Allman, 1986); they are encountered in partially saturated groundwater systems (Wang and Narasimhan, 1985), in geothermal reservoirs (Pruess, 1985), and in oil and gas fields (Dean and Lo, 1986). Modeling of flow in these systems is complicated by the fact that flow geometry may be different for different phases, e.g., for the non-wetting phase flow in the matrix blocks may be local and one-dimensional (toward the fractures or into the blocks), while for the wetting phase there

may be throughflow through the blocks in a global sense.

Rather than going to approximations which are more complex than the double-porosity concept, we pursue in the present paper a much more simplified approach, in which we attempt to approximate fluid and heat flow in a fractured porous medium by means of a single effective or ''equivalent'' continuum. An ''equivalent'' continuum may be defined as one that will yield the same mass fluxes, and temperature, pressure, and saturation distributions as an explicit discrete fracture-porous matrix model, given the same initial and boundary conditions.

Possibilities and limitations for representing the permeability of a fracture system by means of an equivalent porous medium have been studied by Long et al. (1982). These authors have considered steady isothermal single-phase flow in fracture networks, with completely impermeable matrix. The main emphasis of the work by Long et al. was on sparsely fractured systems with fracture density not greatly exceeding the percolation threshold. In contrast, we are dealing with highly fractured flow systems (fracture spacing of the order of 1 ft), where a continuum treatment of fracture permeability on a scale large compared to matrix block sizes appears unproblematic. However, we are interested in processes which involve extensive boiling of formation water in the matrix, so that matrix porosity and permeability cannot be ignored. The main issue then becomes how the interaction between fractures and permeable rock matrix can be accounted for in non-isothermal multi-phase flow.

Our effective continuum approach for describing flow in well-connected fractured-porous media is based on intuitive notions for the behavior of such systems, and on insights gained from detailed numerical simulations (see the companion paper; Part 1, this issue). We present a simple formalism which allows us to compute characteristic curves (relative permeabilities and capillary pressures) for the equivalent continuum in terms of characteristic curves of the matrix and fracture continua, respectively. Results of numerical simulations indicate that under favorable conditions the effective continuum approach can closely approximate the behavior of a fractured porous medium. We also discuss and demonstrate conditions for which the effective continuum approximation breaks down, and derive criteria for its applicability.

The effective continuum concept had been originally introduced in ad hoc fashion (Pruess et al., 1985), in a form that was applicable only to conditions and processes where phase saturations in the fractures remained essentially constant. In this paper we give a more general treatment, which is applicable to the entire range of saturation conditions, from single-phase gas to two-phase gas-liquid to single-phase liquid.

2.0 The Concept of Effective Continuum.

When a fractured porous medium with well-connected fractures and a tight rock matrix is subjected to a hydrologic or thermal perturbation, it will undergo a change in thermodynamic conditions which will tend to propagate rapidly through the fractures but will migrate only slowly into the tight unfractured rock. Because of the different response times of fractures and rock matrix, in general a disequilibrium will evolve in which there may be considerable differences in temperatures and (liquid and gas) phase pressures between fractures and matrix. Also, liquid saturation in the rock matrix will evolve in a non-uniform fashion, because regions deep inside the matrix blocks will be slower to respond to external perturbations than regions near the block surfaces. The magnitude of these differences will depend upon the relative time scales of the external perturbation, and the equilibration process between fractures and rock matrix. This is illustrated in Figures 15 and 16 of the companion paper (Part 1, this issue), which show that with increasing distance from the waste packages matrix blocks tend to respond more uniformly. If the rate of change in thermodynamic conditions caused by the external perturbation is "sufficiently" slow and the equilibration between fractures and rock matrix "sufficiently" rapid, then fractures and rock matrix will remain in approximate thermodynamic equilibrium locally at all times. In this case, the description of the thermohydrologic processes can be simplified considerably, because it is not necessary to keep track of the changes in fracture and matrix conditions separately, the two being linked by local thermodynamic equilibrium. Therefore, one (complete) set of thermodynamic variables will be sufficient to characterize the state of the system locally, and it should then be possible to represent the fractured porous medium by means of a single effective continuum.

From the discussion given above it is clear that the feasibility of an effective continuum description will depend on the nature of the external perturbation, upon the properties of the fractured porous medium, and upon the space- and time-scales of observation. It is an approximation which should never be used indiscriminately but needs to be carefully evaluated for any particular set of circumstances and conditions.

When an effective continuum approximation is applicable, it is necessary to obtain expressions for the effective continuum parameters in terms of properties of the intact matrix rock, and the network of interconnected fractures. Denoting quantities pertaining to fractures with subscript f and to rock matrix with subscript m, we have for a volume V of the system

$$V = V_m + V_f \tag{1}$$

Let ϕ_m be rock matrix porosity, i.e. the void fraction of intact rock, and ϕ_f porosity of the fractures. Under idealized circumstances the fracture domain might be considered to consist entirely of void space (ϕ_f=1); however, ''real'' fractures will in general have considerable roughness and may contain fill, so that ϕ_f<1. The partitioning into matrix and fracture domains is not unique but partly a matter of convenience. For certain analysis it may be advantageous to include wall rock to a certain depth into the ''fracture domain''; in such a case ϕ_f<1 or $\phi_f \ll 1$ is possible (see Table 2 of the companion paper; Part 1, this issue).

We define "equivalent continuum" porosities as the fractions of total volume V that represent voids in matrix and fracture domains, respectively. Thus we have

$$\bar{\phi}_m = \phi_m \frac{V_m}{V} \; (\simeq \phi_m \text{ if } V_f \ll V_m), \text{ and} \tag{2a}$$

$$\bar{\phi}_f = \phi_f \frac{V_f}{V} \; (\simeq \phi_f \, V_f/V_m \text{ if } V_f \ll V_m). \tag{2b}$$

An analogous averaging formula can be used to compute effective continuum liquid saturation S_l in terms of the matrix and fracture saturations, $S_{l,m}$ and $S_{l,f}$:

$$S_l = \frac{S_{l,m}\, \phi_m\, V_m + S_{l,f}\, \phi_f\, V_f}{\phi_m\, V_m + \phi_f\, V_f}. \tag{3}$$

The treatment for effective continuum characteristic curves is considerably more difficult. To obtain useful results, it is necessary to assume that the absolute continuum permeabilities of matrix and fractures can be treated as scalars. In the appendix we show that it is possible to derive an expression for total (liquid or gas) phase flux, which can be interpreted as referring to a single effective continuum with absolute permeability,

$$k = \bar{k}_m + \bar{k}_f \ , \tag{4}$$

and relative permeability,

$$k_\beta = \frac{\bar{k}_m \, k_{\beta,m} + \bar{k}_f \, k_{\beta,f}}{\bar{k}_m + \bar{k}_f} \ . \tag{5}$$

Here $\bar{k}_m$ ($\bar{k}_f$) is the equivalent single-phase continuum permeability of the matrix (fractures) and $k_{\beta,m}$ ($k_{\beta,f}$) is the corresponding relative permeability for phase β (= liquid, gas). Note that different relative permeability functions are expected to apply in matrix and fractures. An equation equivalent to (4) was recently used by Klavetter and Peters for liquid phase flow (Klavetter and Peters, 1986; Peters and Klavetter, 1988).

In these equations, we have defined relative permeabilities relative to total single phase permeability k, so that $0 \le k_\beta \le 1$. Alternatively, the reference continuum permeability may be chosen as $\bar{k}_m$, the permeability of the unfractured rock matrix, so that

$$k = \bar{k}_m, \tag{6}$$

and

$$\hat{k}_\beta = k_\beta \cdot \frac{\bar{k}_m + \bar{k}_f}{\bar{k}_m} = k_{\beta,m} + \frac{\bar{k}_f}{\bar{k}_m} k_{\beta,f}. \tag{7}$$

This is the normalization that was previously chosen by Pruess, Tsang, and Wang (1985). The special approximations for $\hat{k}_\beta$ made in the Pruess et al. paper were possible because $k_{\beta,f}$ remained essentially constant throughout the processes considered.

The quantitative evaluation of the effective continuum relative permeabilities is straightforward. Given a certain average liquid saturation S_l, the corresponding liquid saturations $S_{l,f}$ and $S_{l,m}$ in fractures and matrix can be found from Equation 3 and the

condition of suction equilibrium (see appendix):

$$P_{s,f}\,(S_{l,f}) = P_{s,m}\,(S_{l,m}). \tag{8}$$

Here P_s is the (negative) suction pressure, representing capillary and phase adsorption effects. Knowing the saturations in matrix and fractures, one can evaluate the effective continuum relative permeabilities by explicit computation from Equation 5 or 7. Examples are given in Figures 1 and 2. These refer to the two cases with initially immobile and mobile liquid in the fractures, respectively, which were presented in the companion paper (Part 1, this issue). When plotted on a log-log scale versus gas saturation, it is seen that effective liquid relative permeabilities exhibit a characteristic "double-hump" shape. This is caused by a sharp reduction in liquid permeability in the fractures for rather small average gas saturations. Similar effective liquid phase permeabilities had been proposed previously by Peters and Gauthier (1984), Montazer and Wilson (1984), and Peters and Klavetter (private communication, 1985; 1988). However, these authors did not consider gas phase and non-isothermal effects, and based their model on capillary equilibrium between matrix and fractures.

The approximation of treating permeability as a scalar may or may not be realistic, depending upon fracture geometry and waste package arrangement. For the idealized geometry treated in the companion paper (Figure 1 of Part 1, this issue), this approximation is accurate because for the particular geometry considered the pressure gradient driving global flow is parallel to the fractures.

3.0 Numerical Simulations.

We have applied the formulas given in the previous section to obtain effective continuum parameters for the fractured porous medium considered in the companion paper (Part 1, this issue). Subsequently simulations of thermohydrologic conditions following waste emplacement were carried out for the same initial, boundary, and source conditions as studied in the companion paper. Note that in an effective continuum approximation flow around an infinite linear string of waste packages (Fig. 1 of the companion paper) has one-dimensional cylindrical symmetry. There is no flow between matrix and

fractures in the axial direction, the entire medium being represented as one single continuum. In our computations we used a one-dimensional grid with cylindrical symmetry, which corresponds to one symmetry element of our idealized emplacement configuration. Grid block radii were identical to those used in the explicit fracture calculations (Table 3 of the companion paper). Typical CPU times for effective continuum calculations on a Cray X-MP computer were (Case 1, liquid immobile in fractures) 97.9 s for 5 years physical time, 311.8 s for 100 years, and 358.1 s for 1,000 years. This is comparable to execution times for porous medium calculations without fracture effects, while explicit fracture calculations were slower by a factor of about 20. Results of calculations for backfilled emplacement conditions are given in Figures 3 - 11. Comparison with explicit fracture calculations presented in the companion paper, and with porous medium calculations with no allowance for fracture effects, reveals the following trends.

Overall there is excellent agreement between the explicit fracture and the effective continuum calculations. Temporal and spatial variations of thermodynamic parameters (temperature, pressure, saturation) agree closely while the results obtained from the "no fractures" calculations (unmodified rock matrix parameters) are generally rather different. The effective continuum model can simulate the heat-pipe effect (vapor-liquid counterflow) in a fractured porous medium which keeps the temperature near the heat source near 100°C for a short period of time in Case 1 with liquid immobile in fractures (Fig. 3) and for an indefinitely long time in Case 2 with liquid mobile in fractures. Without taking into account the fractures which are the main conduits for gas-flow from the canister to the ambient rock, the "no fractures" calculations will predict higher temperature near the canister. The effective continuum model also reproduces the saturation and pressure field much better than the "no fractures" calculations (Figs. 4 and 5 for Case 1 and Figs. 8 and 9 for Case 2). It seems particularly significant that gas and liquid flow rates in the effective continuum model show very close agreement with those predicted from the explicit fracture calculations. The flow rates depend on the gradients of the thermodynamic state variables (pressure, temperature, saturation), providing a very sensitive measure of the behavior of the system. Minor quantitative differences between explicit fracture and effective continuum results can be readily understood from

the nature of the approximations made in the effective continuum model. For example, Figure 3 shows that the effective continuum temperatures in Case 1 (liquid immobile in fractures) remain slightly longer near 100°C than predicted from the explicit fracture model. This occurs because in the effective continuum model liquid can vaporize locally, and the vapor generated from boiling immediately has the large fracture permeability available. In the explicit fracture model on the other hand the liquid and/or vapor phases must first flow a short distance (< 11 cm) through the low-permeability matrix. This requires a pressure gradient (see Figure 16 of the companion paper) as well as a temperature gradient between matrix and fractures. Related to this feature is that the heat pipe (vapor-liquid counterflow) process in the effective continuum is slightly more efficient than in the explicit fracture system, because the resistance for matrix-fracture flow is absent in the former. This can be seen in Figures 6, 7 (Case 1) and 10, 11 (Case 2) from the fact that near the inner boundary of the heat pipe mass fluxes in the effective continuum are slightly larger (note the logarithmic scale).

The results given in Figures 3 - 11 substantiate the accuracy of the effective continuum approximation for the early time period of heating and partial drying near the waste packages. Because of the large amount of computing work associated with explicit fracture calculations a comparison with effective continuum predictions could only be made for a rather short time following waste emplacement. We expect the validity of the effective continuum approximation to be process-dependent, so that a verification for a wider range of conditions and parameters is desirable. For example, one may wonder how well the effective continuum approximation will work at later times, e.g., during the process of cooling and resaturation following attainment of peak temperatures.

In order to accomplish an evaluation of the effective continuum approximation for processes and conditions at later time we proceed as follows. We first run an effective continuum calculation out to the time at which a comparison is desired. Then we use the effective continuum results to initialize an explicit fracture calculation, utilizing the assumption of local thermodynamic equilibrium between matrix and fractures to generate the initial conditions. This requires solution of the non-linear Equation (8) with the constraint Eq. (3) for each grid block of the effective continuum model, which is

accomplished by means of Newton-Raphson iteration. Subsequently the problem is restarted in two alternative ways, using either an explicit fracture or an effective continuum approach, so that the desired comparison can be made. An added difficulty here is that at later times all transient changes take place at much smaller rates than in the initial period following waste emplacement, so that the precise level of (dis-) agreement between explicit fracture and effective continuum calculations is much more difficult to ascertain. Further complications arise from somewhat different space- and time-discretization effects in the two models.

We have performed two sets of comparative calculations for backfilled emplacement conditions and Case 1 (liquid immobile in fractures) hydrologic parameters. One set of calculations was initialized at t = 5 yr after waste emplacement, corresponding to the period where formation temperatures and extent of the dried zone approach a maximum. The second set of calculations was initialized at t = 26.28 yr after emplacement, at which time resaturation is taking place in the vicinity of the emplacement hole. In the effective continuum calculation, grid element #3 at a radius of 0.366 m (see Table 3 of the companion paper) is beginning to resaturate at 26.40 yr, or 45.1 days subsequent to restarting at 26.28 yr. Here we will summarize the main features of these calculations with respect to the validity of the effective continuum approximation; the reader interested in a more detailed discussion and comparison of the calculations is referred to a laboratory report (Pruess et al., 1987).

In Figure 12 we have plotted radial heat flow at 5 yr after waste emplacement, and at the end of a subsequent 190.2 day restart period. It is observed that, because of slowly declining heat output from the waste packages (see Figure 9 of the companion paper), heat flow rates during the 190.2 day simulation period decline for $r < 8$ m while they increase at larger distance. In the region of $2.7 \text{ m} < r < 5.5$ m heat transfer is accomplished by a heat pipe mechanism (note the flat temperature profile in this region, Fig. 12), while at smaller and larger distance from the waste packages heat transfer is mainly conductive. In the region interior to the heat pipe, heat flow rates for explicit fractures and effective continuum agree well. Throughout the heat pipe region the effective continuum approximation overpredicts total heat flow by 4% in comparison to the explicit

fracture results, indicating that the effective continuum provides a slightly more efficient heat pipe mechanism than the flow system with explicit fractures. This can also be seen from the total rates of radial liquid flow shown in Figure 13. At the inner boundary of the heat pipe, near r = 2.7 m, inward liquid flow in the effective continuum model is approximately 30% larger than for explicit fractures, while for r > 3 m there is excellent agreement between the two descriptions. As had been pointed out above, the slight difference in heat pipe behavior can be explained in terms of some added flow resistance in the matrix in the explicit fracture model, which is absent in the effective continuum.

The explicit fracture and effective continuum calculations initialized at 26.28 yr after waste emplacement covered a 221.1 day period, showing excellent agreement between the two descriptions with again a slightly more efficient heat pipe in the effective continuum (see Table 1). This causes temperatures in the conduction region interior to the heat pipe to be slightly (1°C) larger in the explicit fracture model. The temperature gradient is approximately 10°C/m near the inner boundary of the heat pipe (r = 3.5 m), so that a 1°C difference in temperature corresponds to a 10 cm difference in effective heat pipe length. This is a small effect indeed considering that total heat pipe length is approximately 4.7 m.

From the calculations presented above we conclude that the effective continuum approximation closely mimics the thermohydrologic behavior of the explicit fracture model for the particular parameters and conditions used. Both descriptions produce the same system behavior, and all fluid and heat flow rates agree to within a few percent everywhere except in a narrow region near the inner boundary of the heat pipe. This slight discrepancy occurs because in the effective continuum approximation the heat pipe mechanism is slightly more efficient, with vapor being able to take advantage of the large fracture permeability without any impedance from the rock matrix.

4.0 Calculations for a Case with Tight Matrix.

Recent measurements have suggested that the value of 32.6 microdarcy used for matrix permeability in the simulations discussed above may be high, and that a value of 1.9 microdarcy may be more representative of the Topopah Spring densely welded tuff

(Braithwaite, personal communication, 1984). For such a tight matrix the process of thermodynamic equilibration between fractures and matrix may be considerably slower, which raises questions about the applicability of an effective continuum approximation.

We have performed explicit fracture and effective continuum calculations for a matrix permeability of 1.9 μd. All other parameters were chosen as in Tables 2 and 3 of the companion paper (Part 1, this issue). Results given in Figures 14 and 15 show that in comparison with explicit fracture calculations the effective continuum approximation overpredicts gas and liquid flow rates by a factor of about 2. The short temperature plateau in the effective continuum model near r = 0.8 m (Fig. 16) indicates the presence of a heat pipe mechanism which because of the low matrix permeability is suppressed in the explicit fracture calculation. These observations as well as a more detailed analysis of the tight matrix calculations in a laboratory report (Pruess et al., 1987) demonstrate that the effective continuum approximation breaks down when the matrix is too tight and approximate local thermodynamic equilibrium cannot be maintained.

5.0 Applicability of Effective Continuum Approximation.

Before applying an effective continuum approximation for modeling thermohydrologic processes in a partially saturated fractured-porous medium it is necessary to establish the validity of the approximation for the conditions under study. One way of doing this is by comparing effective continuum calculations with results obtained for an explicit representation of fractures. However, explicit fracture calculations are tedious and costly, and a simpler means of ascertaining applicability of an effective continuum approximation is desirable.

For the idealized flow geometry considered in the present study (see Fig. 4 of the companion paper; Part 1, this issue) we examine the diffusive processes of gas, liquid, and heat flow in r- as well as z-direction. In radial flow governed by a diffusion equation it is possible to define a "radius of investigation"

$$r_i = 2\sqrt{D_r t} \ , \tag{9}$$

which provides a measure of the radial distance to which a perturbation imposed at t = 0,

$r = 0$ will propagate after time t (Matthews and Russell, 1967). Note that r_i is only an approximate measure because diffusive processes are characterized by broad distributions rather than sharp fronts. The parameter D_r is the diffusivity appropriate for the process under consideration. It is $D_r = K/\rho c$ for heat conduction, and $D_r = k/\phi\beta\mu$ for fluid flow. Here K is thermal conductivity, ρ is density, c is heat capacity, k is permeability, ϕ is porosity, β is compressibility, and μ is fluid viscosity.

Similar considerations can be made for linear diffusive flow perpendicular to the fracture planes. We define a penetration depth

$$z = \sqrt{D_z t} \ , \tag{10}$$

where D_z is the appropriate diffusivity for flow in the matrix perpendicular to the fractures. In a heat conduction problem this corresponds to the depth at which the temperature change in a semi-infinite solid at initially uniform temperature amounts to 48% of a step change imposed at $t = 0$ at the boundary $z = 0$ (Carslaw and Jaeger, 1959).

We are now in a position to develop a criterion for the validity of the effective continuum approximation. Consider a radially symmetric flow system as shown in Figure 4 of the companion paper (Part 1, this issue) being subjected to a perturbation at "small" r at time $t = 0$, which at time t will have propagated to a radius r_i given by Eq. (9). Furthermore, consider a time increment

$$t_L = L^2/D_z \tag{11}$$

for which according to Eq. (10) the diffusive process(es) perpendicular to the fracture plane will penetrate all the way to the center plane of the matrix (fracture spacing 2L).

During the penetration time t_L the radius of investigation will increase by

$$\begin{aligned} \Delta r_i &= 2\left[\sqrt{D_r(t+t_L)} - \sqrt{D_r t}\right] \\ &= r_i\left[\sqrt{1+t_L/t} - 1\right] \ . \end{aligned} \tag{12}$$

An effective continuum approximation should be applicable when the diffusion in z-direction is fast enough so that during the penetration time t_L the advancement Δr_i of the radial diffusion is "small." This leads us to propose the following condition as being

sufficient to ensure validity of the effective continuum approximation:

$$\Delta r_i \ll r_i \quad . \tag{13}$$

From Eqs. (11) and (12) this can be rewritten as

$$t \gg L^2/D_z \quad . \tag{14}$$

Alternatively, using Eq. (9) the criterion can be stated in terms of the radius of investigation

$$r_i \gg 2L\sqrt{D_r/D_z} \quad . \tag{15}$$

Based on the above derivation, either of Eq. (14) or (15) should provide a sufficient criterion for the applicability of an effective continuum approximation. Note that, regardless of the applicable thermal and hydrologic parameters, an effective continuum approximation will be valid at "sufficiently" large times or radial distances. At this point we have not attached a precise quantitative meaning to the inequalities (14) and (15). Diffusive processes are characterized by very broad fronts, so that it is not clear by what factors time or distance should exceed the above estimates to provide for "approximate" local equilibrium between matrix and fractures.

We wish to point out the analogy between a fractured porous medium and a layered formation. It is well known that the pressure responses in different layers of an aquifer converge towards a uniform behavior for sufficiently large times and distances (Javandel, 1968).

In order to apply the criteria derived above it is necessary to identify the diffusivities to be used in Eqs. (14) and (15). For D_r the diffusivity corresponding to heat conduction is appropriate, as this provides the mechanism for radial propagation of the imposed perturbation. It is not quite so clear what the appropriate choice for D_z should be, because the interchange between matrix and fractures involves two-component two-phase fluid flow as well as heat conduction. In two-phase systems compressibility can become a very complex parameter, because pressure propagation is coupled to temperatures which are buffered by the heat content of the solid (Sorey et al., 1980). For the present problem we believe that the most appropriate diffusivities for characterizing flow

in the matrix perpendicular to the fractures are the diffusivities for single-phase gas flow, and for single-phase capillary-driven liquid flow. The reason for this is that because of the predominantly radial heat flow, temperatures at a given radial distance r do not depend strongly on the location z in the matrix. Certainly when an effective continuum approximation is applicable temperatures and pressure will depend primarily on radius r, being only weakly dependent on z. Then most phase change effects will take place near the matrix-fracture interface.

Diffusivities for the thermal and hydrologic parameters used in our simulations (see Table 2 of the companion paper; Part 1, this issue) are given in Table 2. Note that the diffusivities for liquid and gas flow are of similar magnitude. They are larger than the thermal diffusivity for the calculations with large matrix permeability (32.6 μd), but are smaller in the case of a tight matrix (1.94 μd). Taking $D_r = 8.16 \times 10^{-7}$ m^2/s and using for D_z the smaller of the gas and liquid diffusivities, inequalities (14) and (15) for the validity of the effective continuum approximation take on the following form:

(a) for large matrix permeability (32.6 μd)

$$t >> 4583 \text{ s, or } 0.053 \text{ days}$$

$$r_i >> 0.122 \text{ m; and}$$

(b) for tight matrix (1.94 μd)

$$t >> 7.71 \times 10^4 \text{ s, or } 0.89 \text{ days}$$

$$r_i >> 0.502 \text{ m}.$$

Our comparisons between effective continuum and explicit fracture calculations were made at a time of 160 days (or larger) for the case with large matrix permeability, and at a time of 36.5 days for the tight matrix case. These times exceed the right hand side in the above inequalities for time by factors of 3016 (or more) and 40.9,

respectively. The excellent agreement between effective continuum and explicit fracture calculations observed for the case with large matrix permeability (Figs. 3-13) indicates that a factor of order 3000 in the time inequality is "sufficiently" large, while for a factor of order 40 significant deficiencies of the effective continuum approximation are apparent (Figs. 14-16). Because of the general form of the time-distance relationship in linear diffusion (Eqs. 9,10) we expect that the inequality factors in the space domain should scale like the square roots of the corresponding factors in the time domain.

6.0 Discussion and Conclusions

In this paper we have presented an effective continuum approximation for modeling fluid and heat flow in variably-saturated fractured-porous media. This approximation is based on the concept of approximate local thermodynamic equilibrium between rock matrix and fractures. Where applicable it provides a drastic simplification of flow problems which makes it possible to perform simulations over large space- and time-scales. Formulas were derived for expressing effective continuum parameters in terms of matrix and fracture data.

Through comparisons with calculations in which fractures were represented explicitly it was demonstrated that the effective continuum approximation gave very accurate results in a case with "large" rock matrix permeability (32.6 μd), but gave poor results for the small space- and time-scales investigated in a case with "tight" matrix (1.9 μd). It is clear, therefore, that the validity of the approximation depends on the particular parameters and conditions present in a flow system.

Considerations of "global" diffusivities as well as diffusivities for "local" interporosity flow between matrix and fractures lead to general approximate criteria for the validity of an effective continuum approximation. These criteria were shown to be consistent with the results of our numerical simulations. Generally speaking, the effective continuum approximation will break down for processes involving rapid transients, and for conditions of very tight rock matrix or large fracture spacing. The diffusivities to be applied for evaluating the validity of the effective continuum approximation are specific to the process under study. For example, if a variably-saturated fractured-porous system

initially at steady state is perturbed by means of heat input the diffusivity to be used for global flow is that corresponding to heat conduction, while in a case where the external perturbation consists of water infiltration into fractures a diffusivity corresponding to liquid flow in fractures will have to be used.

It should be emphasized that regardless of applicable diffusivities an effective continuum approximation will be applicable when "sufficiently" large space- and time-scales are considered. The estimates for these scales given in Section 5 have important practical applications for numerical simulations. Whenever space- or time-discretization is chosen coarse enough to meet the criteria for validity of an effective continuum approximation its application is justified. With coarse discretization one simply fails to resolve details on smaller scales on which deviations from the effective continuum approximation could be seen.

The effective continuum approximation was used in recent simulation studies of repository-wide gas phase convection effects by Tsang and Pruess (1987). The smallest volume element in their computational grid had a volume of 2.4×10^5 m^3, corresponding to an average linear dimension of more than 60 m for the smallest grid block. This is large compared to the estimates given in Section 5, so that on the scale considered an effective continuum approach was justified even for the tight matrix case.

Acknowledgement

This work was supported by the Yucca Mountain Project, Sandia National Laboratories, and the U.S. Department of Energy under Contract No. DE-AC03-76SF00098. For a critical review of the manuscript and the suggestion of improvements the authors are indebted to C. Doughty, S. Benson, S. Passman, A. Treadway, and B. Langkopf.

References

Barenblatt, G. E., Zheltov, I. P., and Kochina, I. N., Basic concepts in the theory of seepage of homogeneous liquids in fissured rocks, J. Appl. Math., (USSR), Vol. 24, No. 5, pp. 1286-1303, 1960.

Carslaw, H. S., and Jaeger, J. C., Conduction of Heat in Solids, Oxford University Press, Oxford, England, Second Edition, 1959.

Dean, R. H., and Lo, L. L., Development of a natural fracture simulator and examples, paper SPE-14110, presented at the SPE 1986 International Meeting on Petroleum Engineering, Beijing, China, March 1986.

Javandel, I., Analysis of transient fluid flow in multi-layered systems, Ph.D dissertation, University of California, Berkeley, CA, 1968.

Klavetter, E., and Peters, R. R., Fluid flow in a fractured rock mass, Sandia National Laboratories, Report SAND85-0855, Albuquerque, NM, March 1986.

Long, J. C. S., Remer, J. S., Wilson, C. R., and Witherspoon, P. A., Porous media equivalents for networks of discontinuous fractures, Water Resources Research, Vol. 18, No. 3, pp. 645-658, June 1982.

Matthews, C. S., and Russel, D. G., Pressure Buildup and Flow Tests in Wells, Society of Petroleum Engineers, Monograph Vol. 1, New York, 1967.

Miller, J. D., and Allman, D. W., Dual permeability modeling of flow in a fractured geothermal reservoir, Proceedings, Eleventh Workshop Geothermal Reservoir Engineering, Stanford University, Stanford, CA., pp. 77-84, January 1986.

Moench, A. F., Well test analysis in naturally fissured, geothermal reservoirs with fracture skin, Proceedings, Ninth Workshop on Geothermal Reservoir Engineering, Stanford University, Stanford, CA., December 1983.

Montazer, P., and Wilson, W. E., Conceptual hydrologic model of flow in the unsaturated zone, Yucca Mountain, Nevada, U.S. Geological Survey, Water Resources Investigations Report 84-4345, Lakewood, Colorado, 1984.

Peters, R. R., and Gauthier, J. H., Results of TOSPAC calculations for Yucca Mountain, Unpublished memo to F. W. Bingham, April 30, 1984.

Peters, R. R. and Klavetter, E. A., A continuum model for water movement in an unsaturated fractured rock mass, Water Resources Res., Vol. 24, No. 3, pp. 416-430, 1988.

Pruess, K., A quantitative model of vapor dominated geothermal reservoirs as heat pipes in fractured porous rock, Geothermal Resources Council, Transactions, Vol. 9, part II, pp. 353-361, August 1985.

Pruess, K., and Narasimhan, T. N., On fluid reserves and the production of superheated steam from fractured, vapor-dominated geothermal reservoirs, Journal of Geophysical Research, Vol. 87, No. B11, pp. 9329-9339, 1982.

Pruess, K., and Narasimhan, T. N., A practical method for modeling fluid and heat flow in fractured porous media, Society of Petroleum Engineers Journal, Vol. 25, No. 1, pp. 14-26, February 1985.

Pruess, K., Tsang, Y. W., and Wang, J. S. Y., Modeling of strongly heat driven flow in partially saturated fractured porous media, International Association of Hydrogeologists (ed.), Memoires, Vol. XVII, pp. 486-497, 1985.

Pruess, K., Wang, J. S. Y., and Tsang, Y. W., Effective continuum approximation for modeling fluid and heat flow in fractured porous tuff, Sandia National Laboratories, Report SAND 86-7000, Albuquerque, NM, 1987.

Sorey, M. L., Grant, M. A., and Bradford, E., Nonlinear effects in two-phase flow to wells in geothermal reservoirs, Water Resources Research, Vol. 16, No. 4, pp. 767-777, August 1980.

Tsang, Y. W., and Pruess, K., A study of thermally induced convection near a high-level nuclear waste repository in partially saturated fractured tuff, Water Resources Research, Vol. 23, No. 10, pp. 1958-1966, 1987.

Wang, J. S. Y. and Narasimhan, T. N., Hydrologic mechanisms governing fluid flow in a partially saturated, fractured, porous medium, Water Resources Res., Vol. 21, No. 12, pp. 1861-1874, December 1985.

Warren, J. E., and Root, P. J., The behavior of naturally fractured reservoirs, Soc. Pet. Eng. J., pp. 245-255, September 1963. (also: Transactions, AIME, 228.)

Appendix: Characteristic Curves for an Effective Continuum

Let us consider two-phase flow in a fractured porous medium. We write Darcy's law in the following form:

$$\mathbf{F}_{\beta,\mathrm{matrix}} = -\bar{k}_m \, k_{\beta,m} \left[\frac{\rho_\beta}{\mu_\beta}\right]_m (\nabla P_{\beta,m} - \rho_{\beta,m}\, \mathbf{g}) \; ; \tag{A.1}$$

$$\mathbf{F}_{\beta,\mathrm{fractures}} = -\bar{k}_f \, k_{\beta,f} \left[\frac{\rho_\beta}{\mu_\beta}\right]_f (\nabla P_{\beta,f} - \rho_{\beta,f}\, \mathbf{g}) \, . \tag{A.2}$$

The notation is

$\mathbf{F}$	= mass flux
β	= phase index (β = liquid, gas)
subscript m	= relating to matrix
subscript f	= relating to fractures
$\bar{k}_m$ ($\bar{k}_f$)	= equivalent single phase continuum permeability of matrix (fractures)
$k_{\beta,m}$ ($k_{\beta,f}$)	= relative permeability to phase β in matrix (fractures)
ρ_β	= density of phase β
μ_β	= viscosity of phase β
P_β	= pressure of phase β
$\mathbf{g}$	= acceleration of gravity.

The flux expressions given above should not be considered ''point'' quantities, but represent averages over a suitably chosen area. This area may be thought of as an interface area between grid blocks in a discretized description of flow (with grid block volumes being equal to or larger than an REV). Requiring approximate local thermodynamic equilibrium between matrix and fractures, we have

(1) equality of temperatures,

$$T_m = T_f \; ; \tag{A.3}$$

and

(2) equality of phase pressures,

$$P_{\beta,m} = P_{\beta,f} \quad (\beta = \text{liquid, gas}). \tag{A.4}$$

More explicitly, the pressure condition can be written

$$P_{g,m} = P_{g,f} \tag{A.4a}$$

$$P_{l,m} = P_{l,f} \; . \tag{A.4b}$$

Noting that $P_l - P_g = P_s$ is the suction pressure in the liquid phase (representing capillary and phase adsorption effects), subtraction of the gas pressure equation from that for liquid gives equality of suction pressures in matrix and fractures:

$$P_{s,m} = P_{s,f} \; . \tag{A.5}$$

Under conditions of (local) thermodynamic equilibrium we also have $\rho_{\beta,m} = \rho_{\beta,f}$ and $\mu_{\beta,m} = \mu_{\beta,f}$ so that addition of the fluxes for matrix and fractures gives the following expression for total flux (note that equality of pressures implies equality of pressure gradients):

$$\begin{aligned} \mathbf{F}_\beta &= \mathbf{F}_{\beta,\text{matrix}} + \mathbf{F}_{\beta,\text{fractures}} \\ &= -(\bar{k}_m \, k_{\beta,m} + \bar{k}_f \, k_{\beta,f}) \frac{\rho_\beta}{\mu_\beta} (\nabla P_\beta - \rho_\beta \, \mathbf{g}). \end{aligned} \tag{A.6}$$

Here the relative permeabilities $k_{\beta,m}$ and $k_{\beta,f}$ have to be evaluated at saturations $S_{\beta,m}$ and $S_{\beta,f}$, respectively, such that $P_{s,m}(S_{\beta,m}) = P_{s,f}(S_{\beta,f})$.

The expression for total flux can be interpreted as referring to a single effective continuum with total effective phase permeability of $\bar{k}_m \, k_{\beta,m} + \bar{k}_f \, k_{\beta,f}$. For single phase flow, the effective continuum permeability becomes $k = \bar{k}_m + \bar{k}_f$, so that the effective continuum relative permeability can be defined as

$$k_\beta = \frac{\bar{k}_m \, k_{\beta,m} + \bar{k}_f \, k_{\beta,f}}{\bar{k}_m + \bar{k}_f} . \tag{A.7}$$

The total phase flux is then given by the following single continuum expression:

$$F_\beta = - k \, k_\beta \frac{\rho_\beta}{\mu_\rho} \left(\nabla P_\beta - \rho_\beta \, g \right) . \tag{A.8}$$

Table 1. Vapor Flow Rates in Heat Pipe Region at 26.89 yr

Distance (m)	Rate of Outward Vapor Flow (kg/s)	
	Explicit Fractures	Effective Continuum
3.56	1.72×10^{-4}	2.57×10^{-4}
4.46	6.93×10^{-4}	7.03×10^{-4}
5.52	7.40×10^{-4}	7.41×10^{-4}
6.74	7.45×10^{-4}	7.48×10^{-4}
8.18	7.71×10^{-5}	8.43×10^{-5}

Table 2. Diffusivities for Fluid and Heat Flow Processes.

process	parameters	diffusivity (m^2/s)
heat conduction	$K = 1.6$ W/m°C $\rho = 2550$ kg/m^3 $C_R = 768.8$ J/kg°C	8.16×10^{-7}
single-phase gas flow	$k_m = 32.6 \times 10^{-18}$ m^2 $\phi_m = 10.3$ % $\beta \approx 1/P \approx 10^{-5}$ Pa^{-1} $\mu = 1.2 \times 10^{-5}$ Pa·s*	2.64×10^{-6}
--, tight matrix	$k_m = 1.94 \times 10^{-18}$ m^2	1.57×10^{-7}
unsaturated liquid flow	$k_m = 32.6 \times 10^{-18}$ m^2 $\phi_m = 10.3$ % $\beta \approx dS_l/dP_{cap} = 2.34 \times 10^{-7}$ Pa^{-1} † $\mu_l = 2.79 \times 10^{-4}$ Pa·s‡	4.85×10^{-6}
--, tight matrix	$k_m = 1.94 \times 10^{-18}$ m^2	2.89×10^{-7}

* vapor at T = 100°C

† at initial saturation $S_l = 80\%$

‡ at T = 100°C

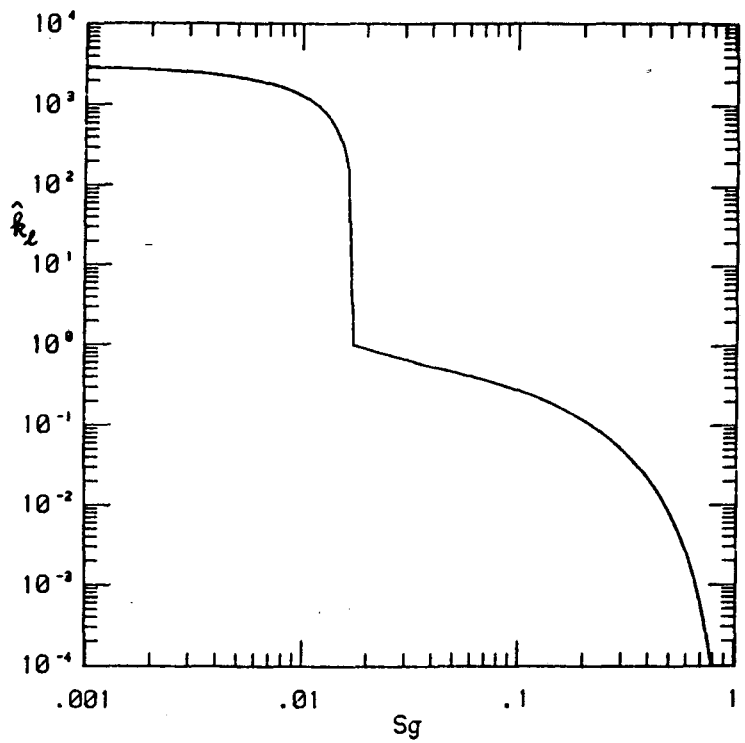

XBL 8511-4792

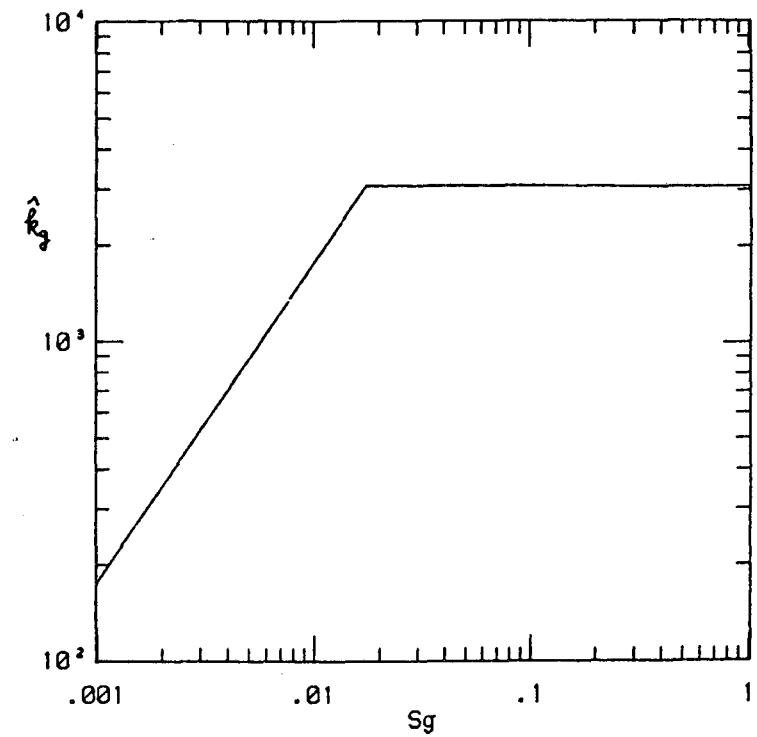

XBL 8511-4791

Figure 1. Effective continuum relative permeabilities for a case with liquid immobile in fractures (a-liquid, b-gas). The parameters are given in the companion paper (Part 1, this issue).

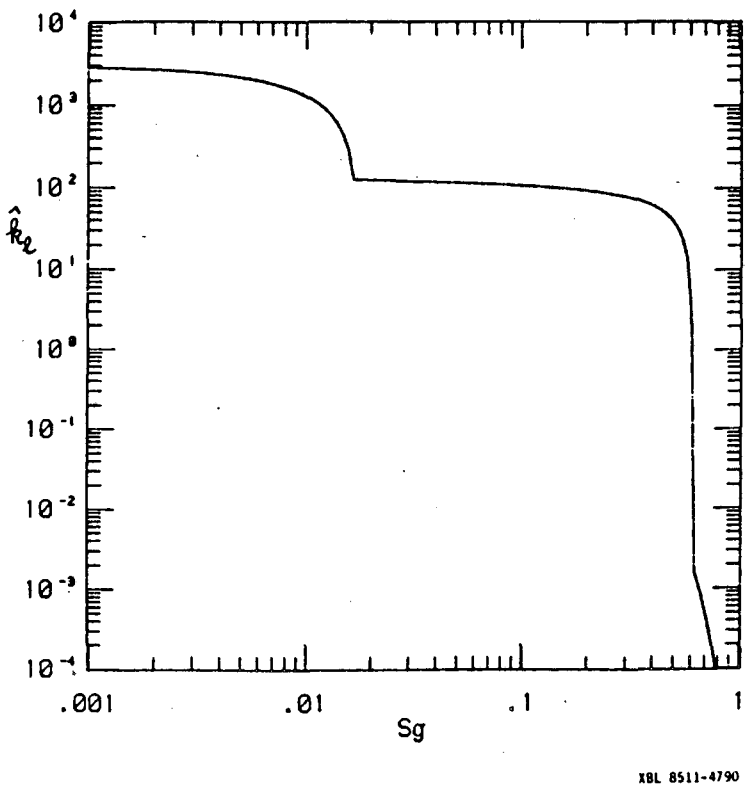

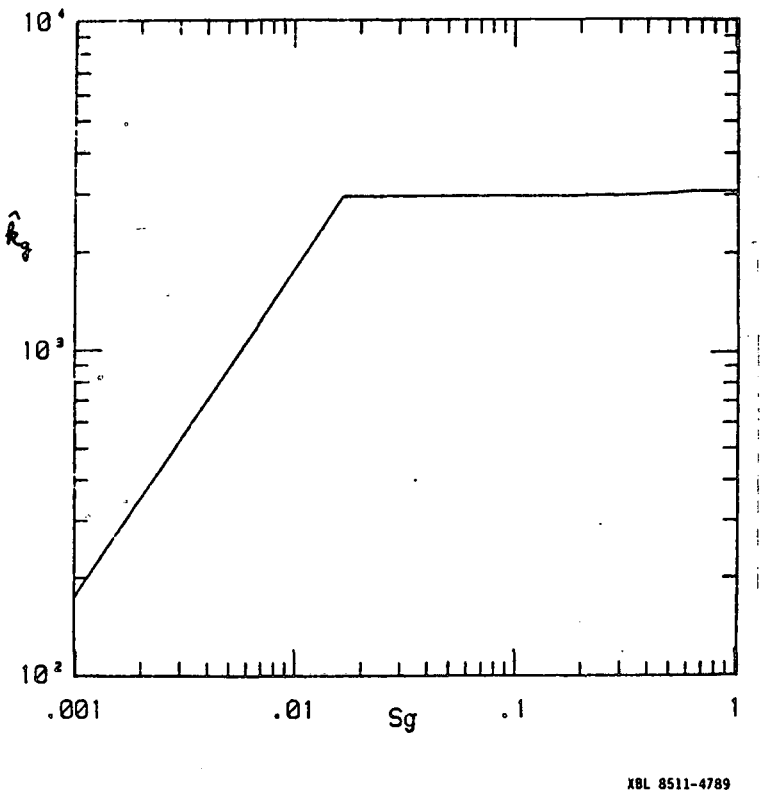

Figure 2. Effective continuum relative permeabilities for a case with liquid mobile in fractures (a-liquid, b-gas).

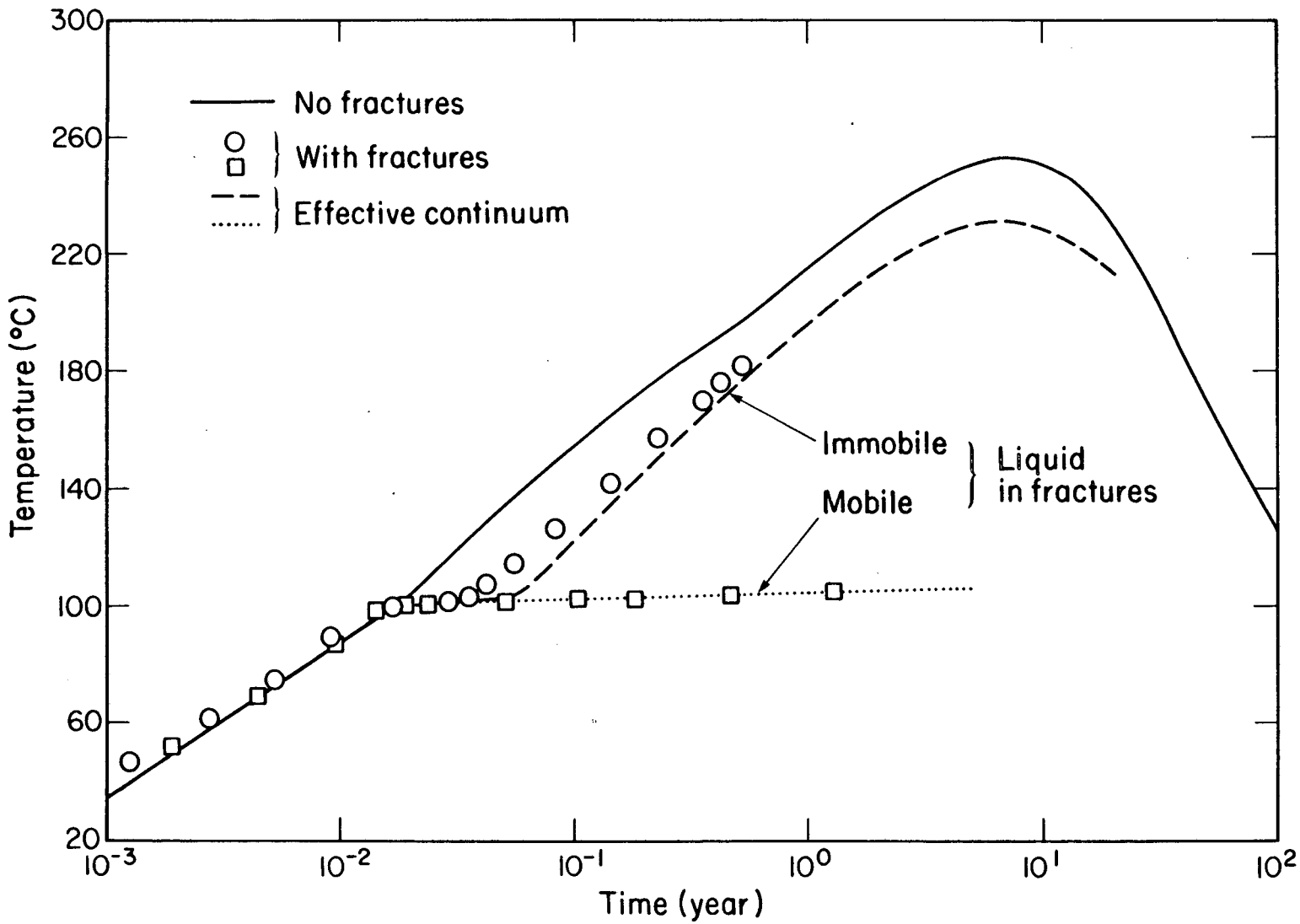

Figure 3. Simulated temperatures at a distance of 0.34 m from the centerline of the waste packages for backfilled emplacement conditions.

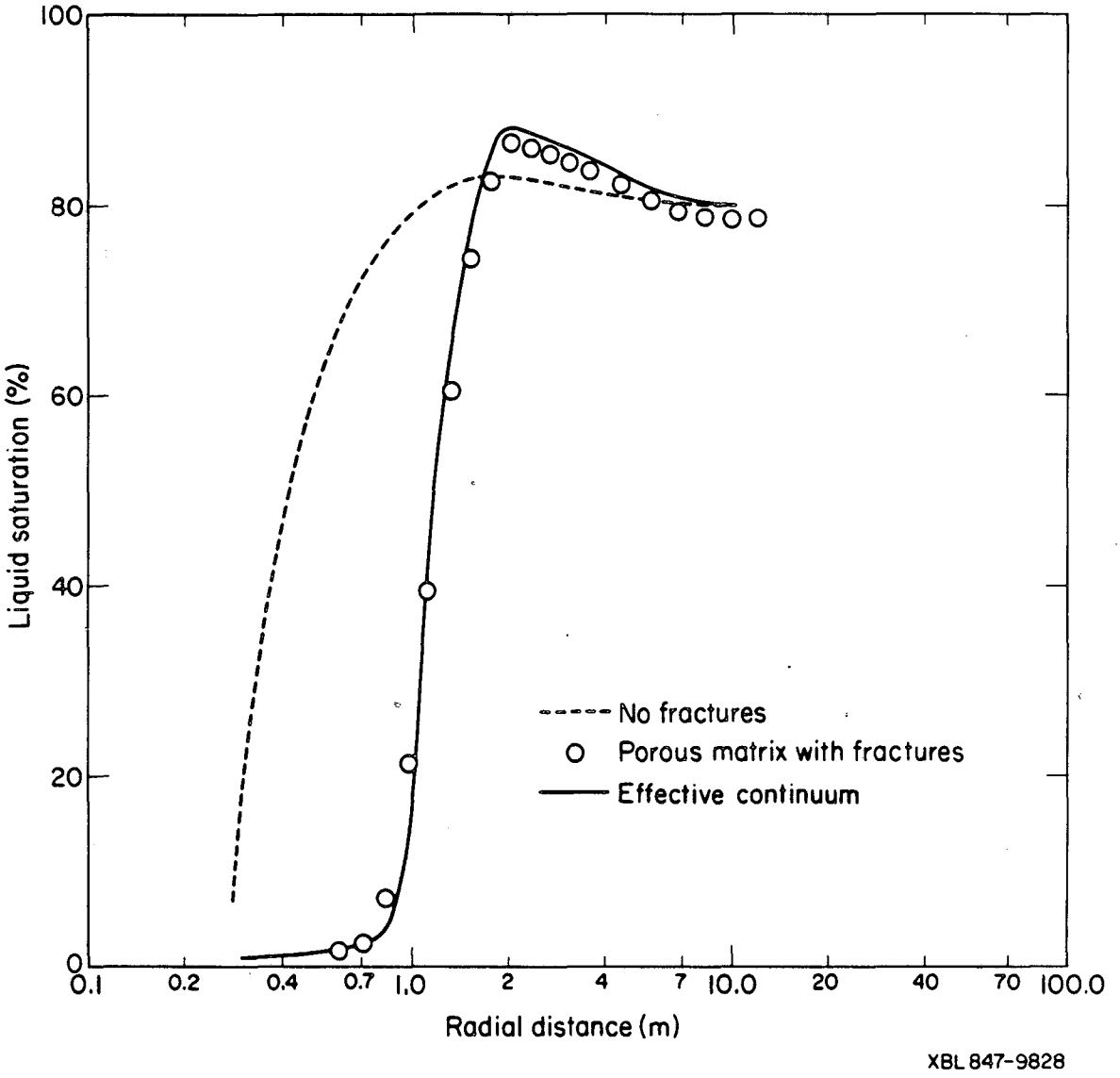

Figure 4. Liquid saturation distribution at 160 days after waste emplacement (Case 1 - liquid immobile in fractures; data for "porous matrix with fractures" are averages over the matrix domain).

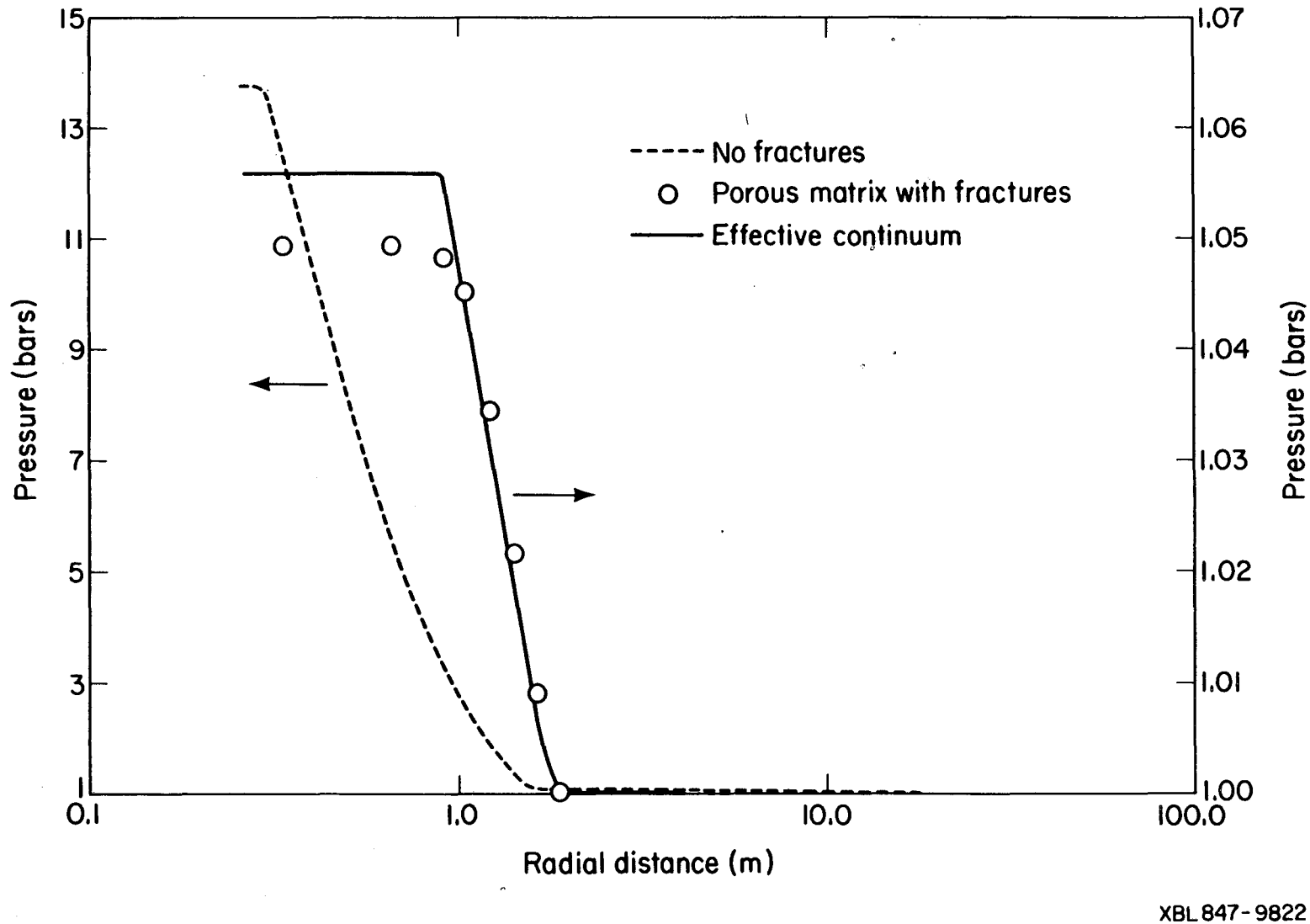

Figure 5. Pressure profiles at 160 days after waste emplacement (Case 1; for the "porous matrix with fractures" the pressures in the fractures are plotted; note the different scales!).

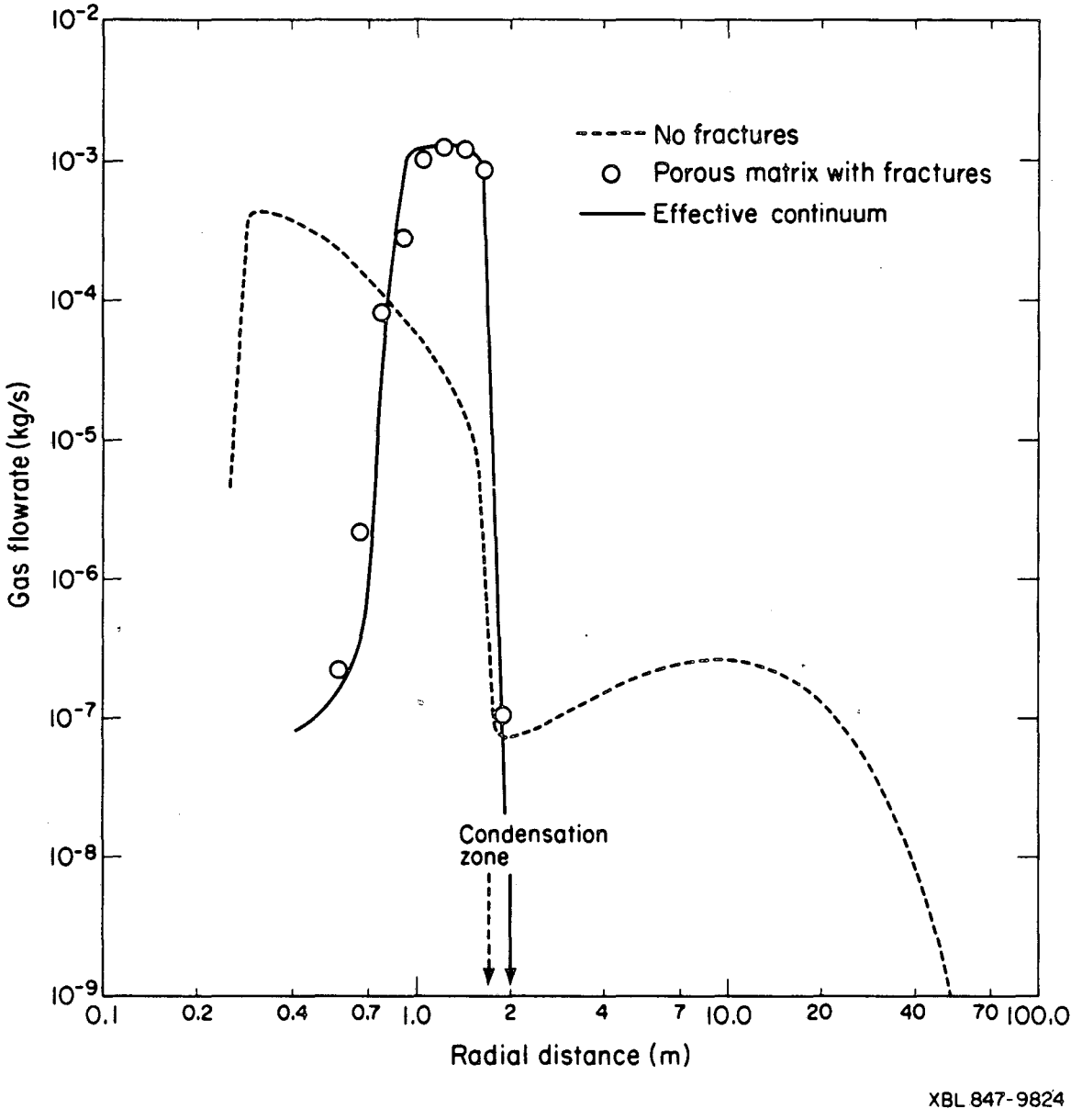

Figure 6. Simulated rates of radial gas flow per waste package at 160 days after emplacement (Case 1).

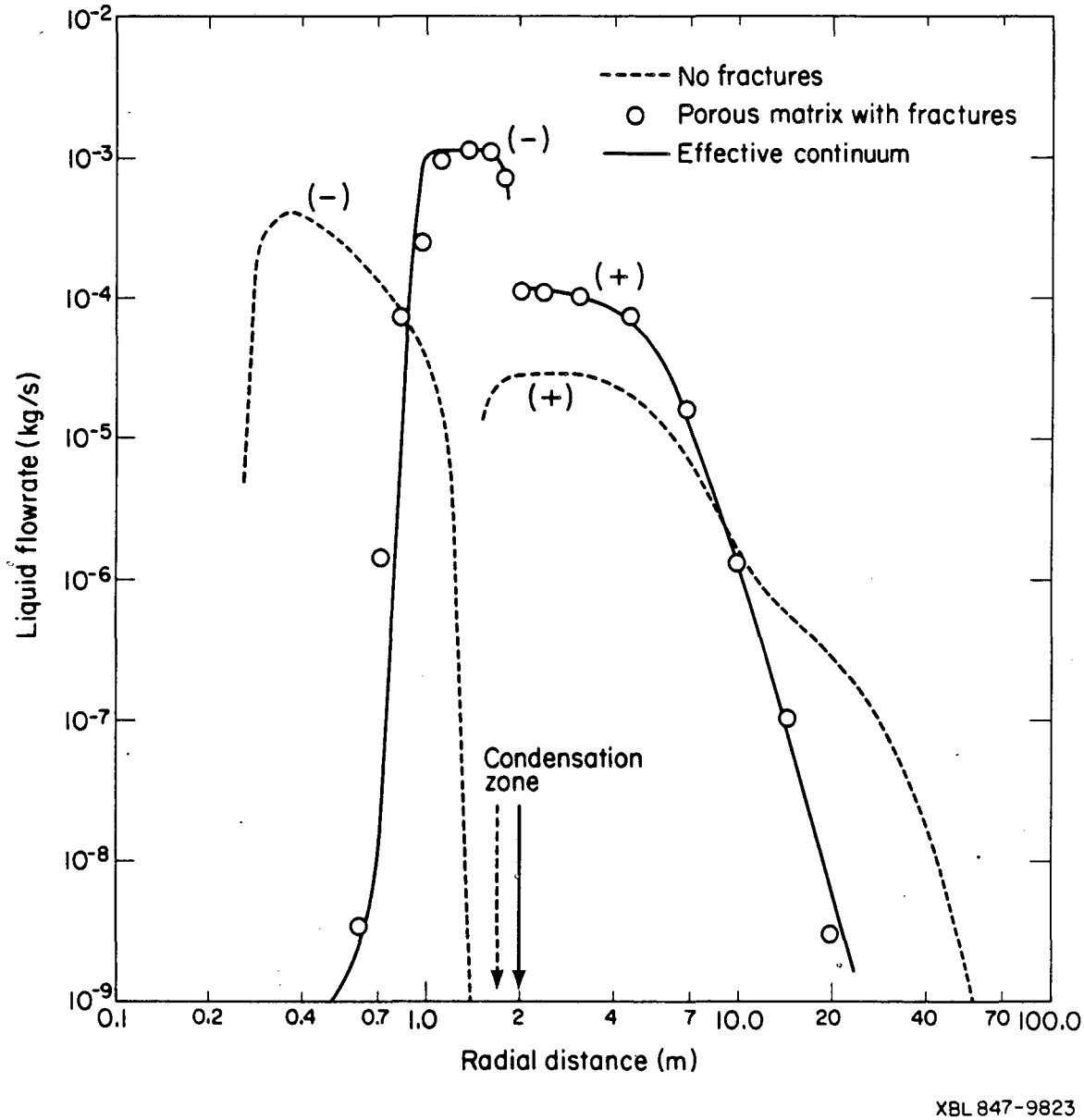

Figure 7. Rates of radial liquid flow per waste package at 160 days after emplacement (Case 1; a "-" sign indicates flow toward the waste packages).

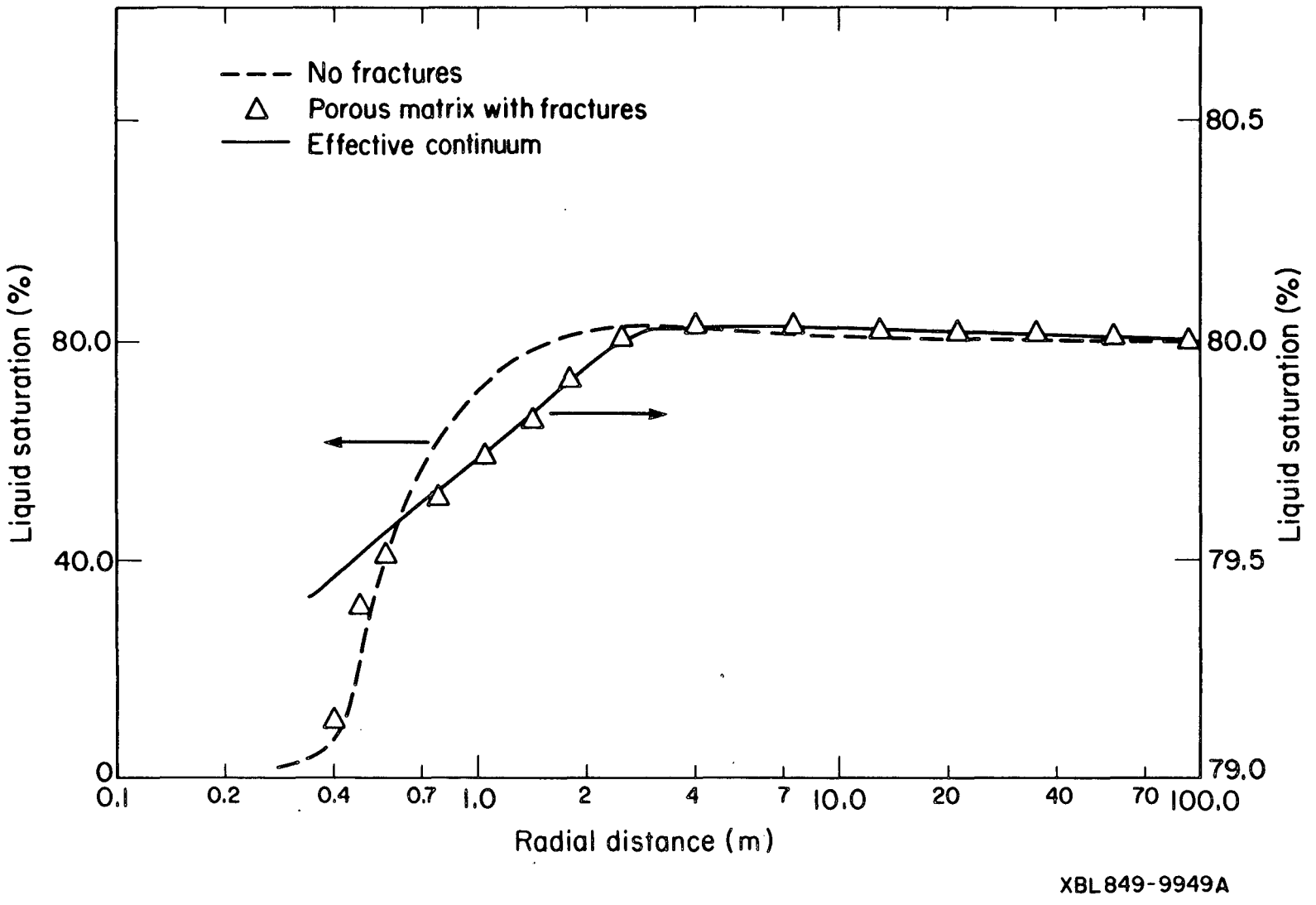

Figure 8. Liquid saturation distribution at 1 yr after waste emplacement (Case 2 - liquid mobile in fractures; note the different scales. Data for "porous matrix with fractures" are averages over the matrix domain).

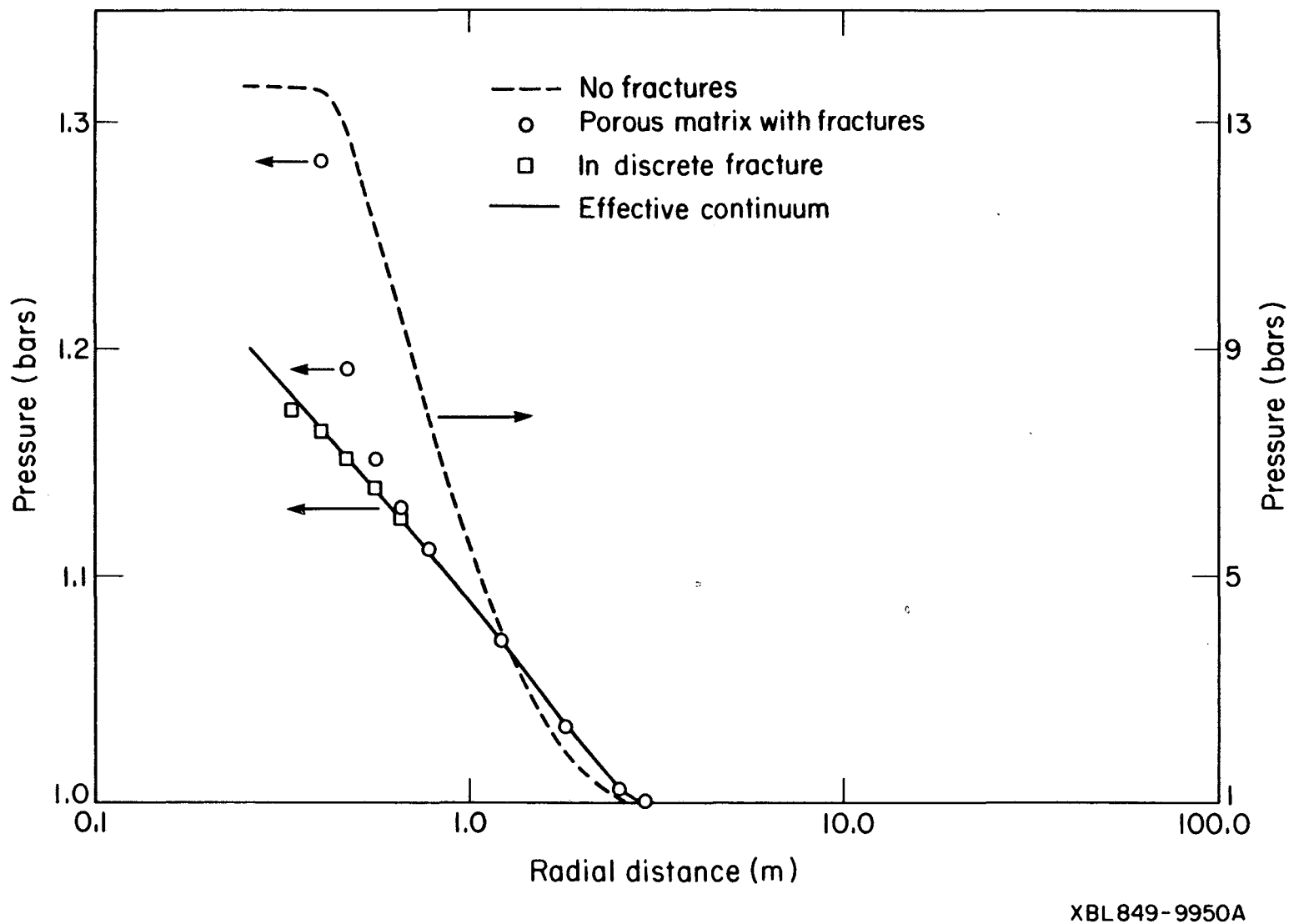

Figure 9. Pressure profiles at 1 yr after waste emplacement (Case 2; note the different scales!).

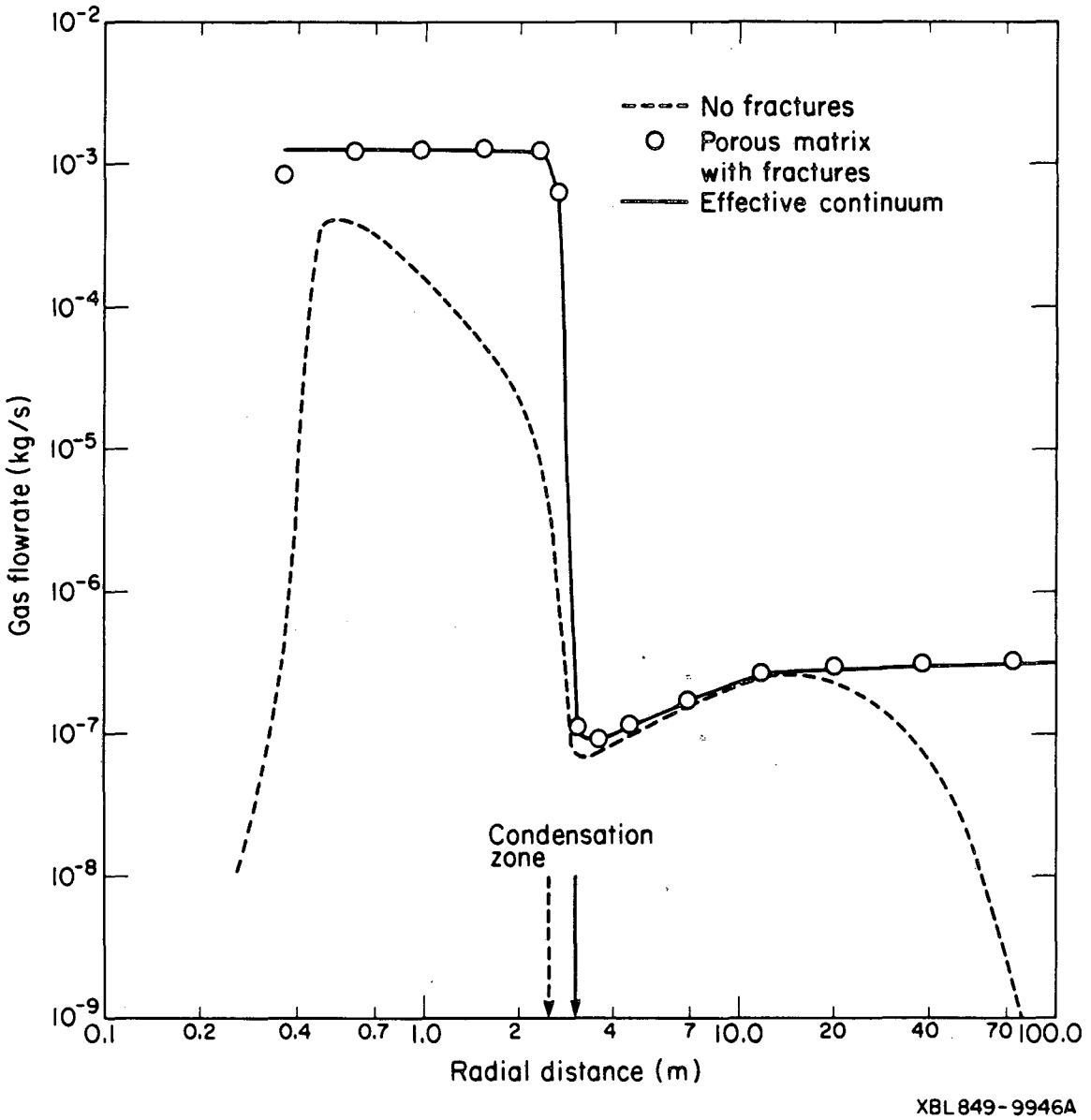

Figure 10. Rates of radial gas flow per waste package at 1 yr after emplacement (Case 2).

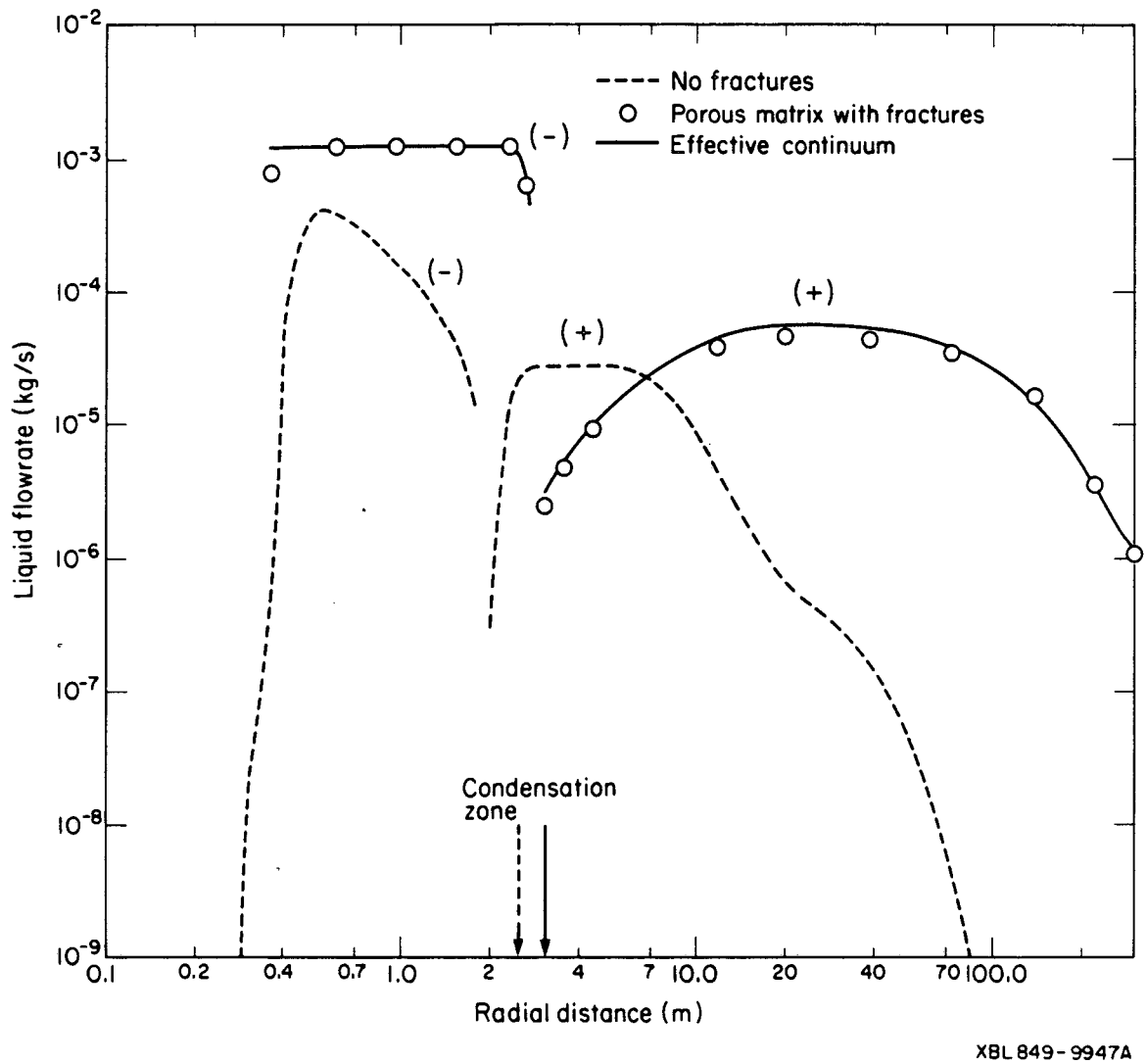

Figure 11. Rates of radial liquid flow per waste package at 1 yr after emplacement (Case 2; a "-" sign indicates flow toward the waste packages).

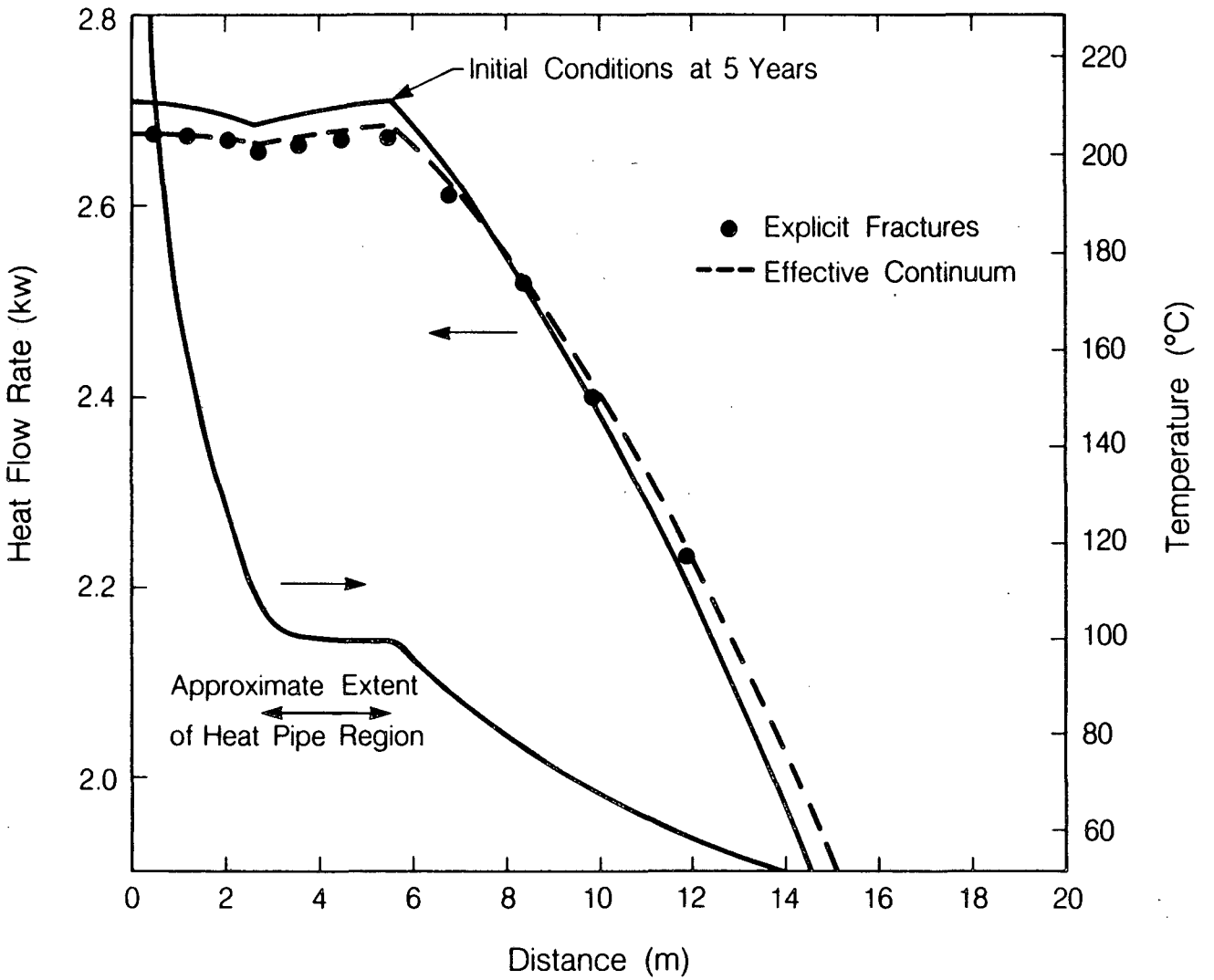

XBL 8511-12622

Figure 12. Rates of radial heat flow per waste package at 5 yr and 5 yr + 190.2 days (Case 1 - liquid immobile in fractures; backfilled emplacement conditions). The temperature profile at 5 yr after emplacement is also shown.

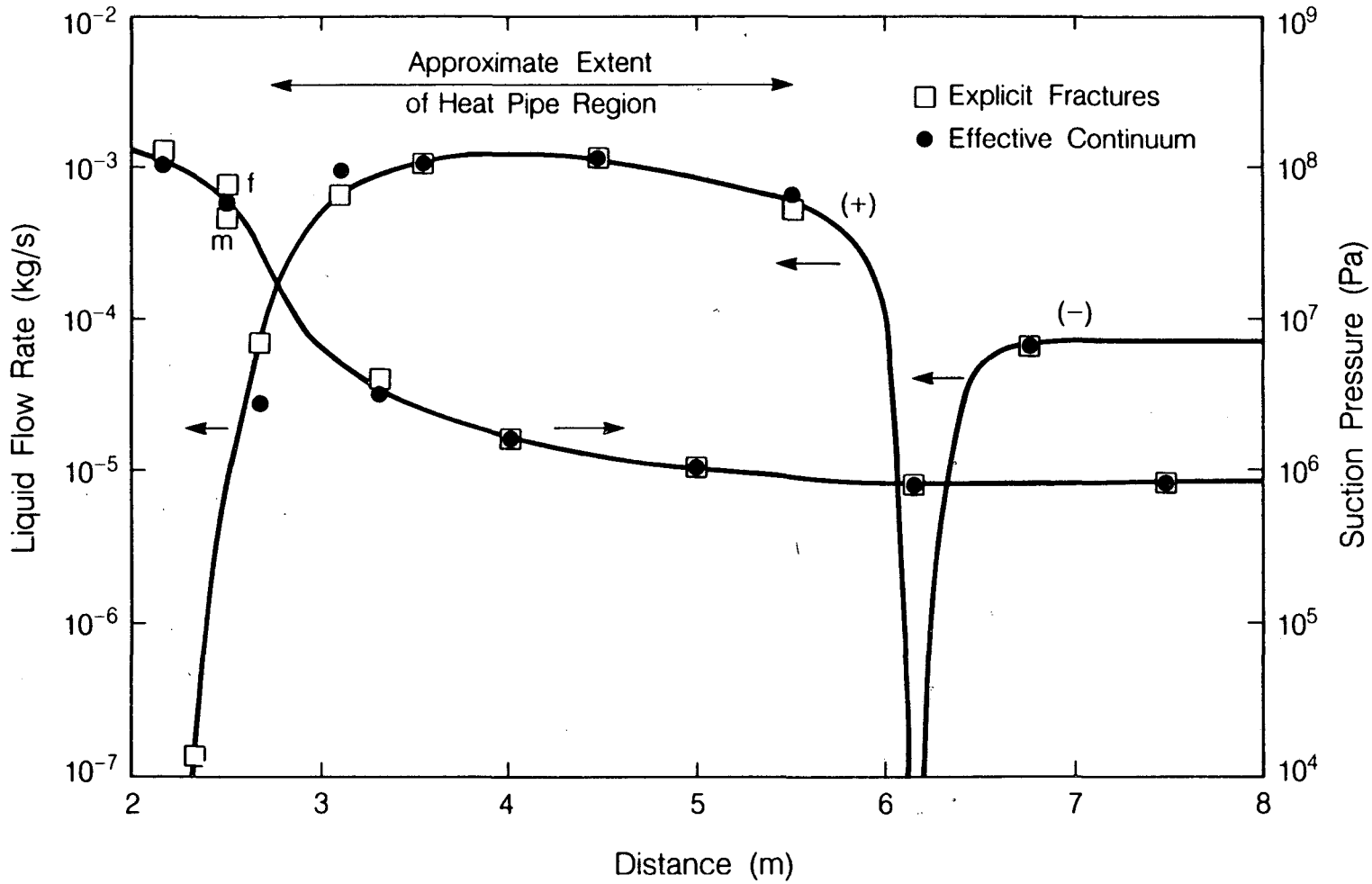

Figure 13. Rates of radial liquid flow and suction pressures at 5 yr + 190.2 days (Case 1; backfilled emplacement conditions; points labeled "f" and "m" represent fracture and innermost matrix regions. The solid lines are eye-fits).

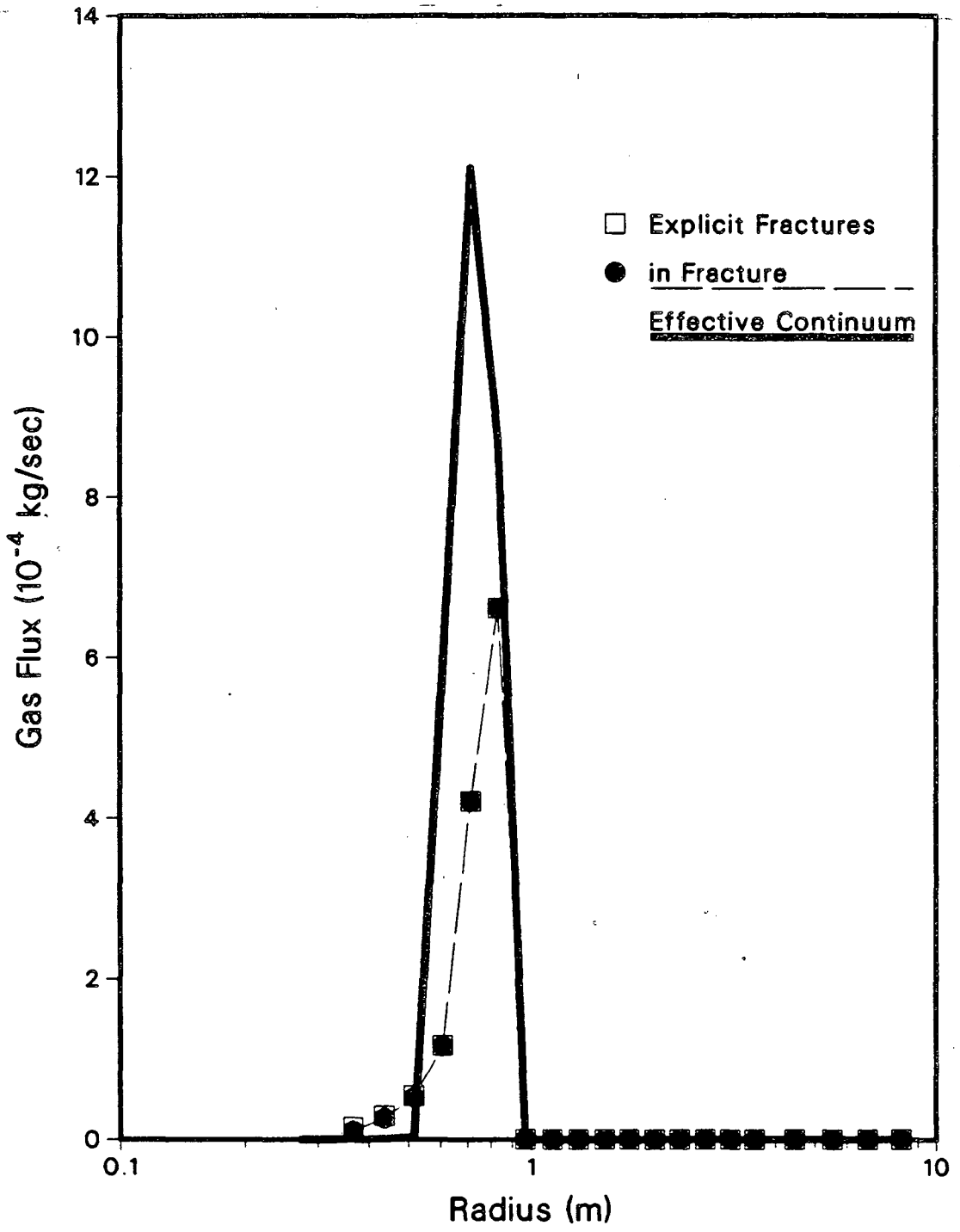

XBL 878-3629

Figure 14. Rates of radial gas flow at 36.5 days (''tight'' matrix; backfilled emplacement conditions; the points labeled "explicit fractures" represent total radial flow, summed over matrix and fracture).

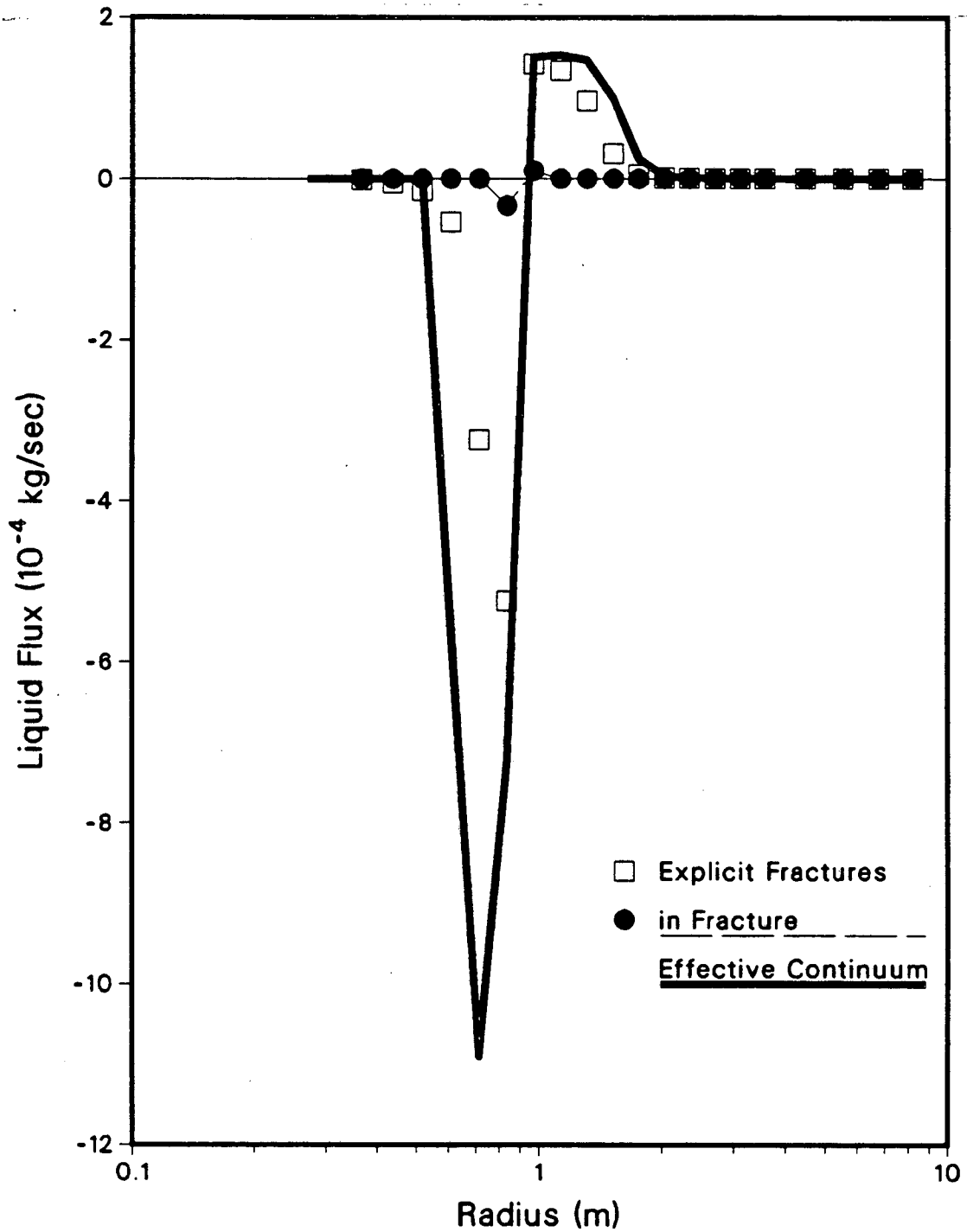

XBL 878-3628

Figure 15. Rates of radial liquid flow at 36.5 days (''tight'' matrix; backfilled emplacement conditions; the points labeled "explicit fractures" represent total radial flow, summed over matrix and fracture).

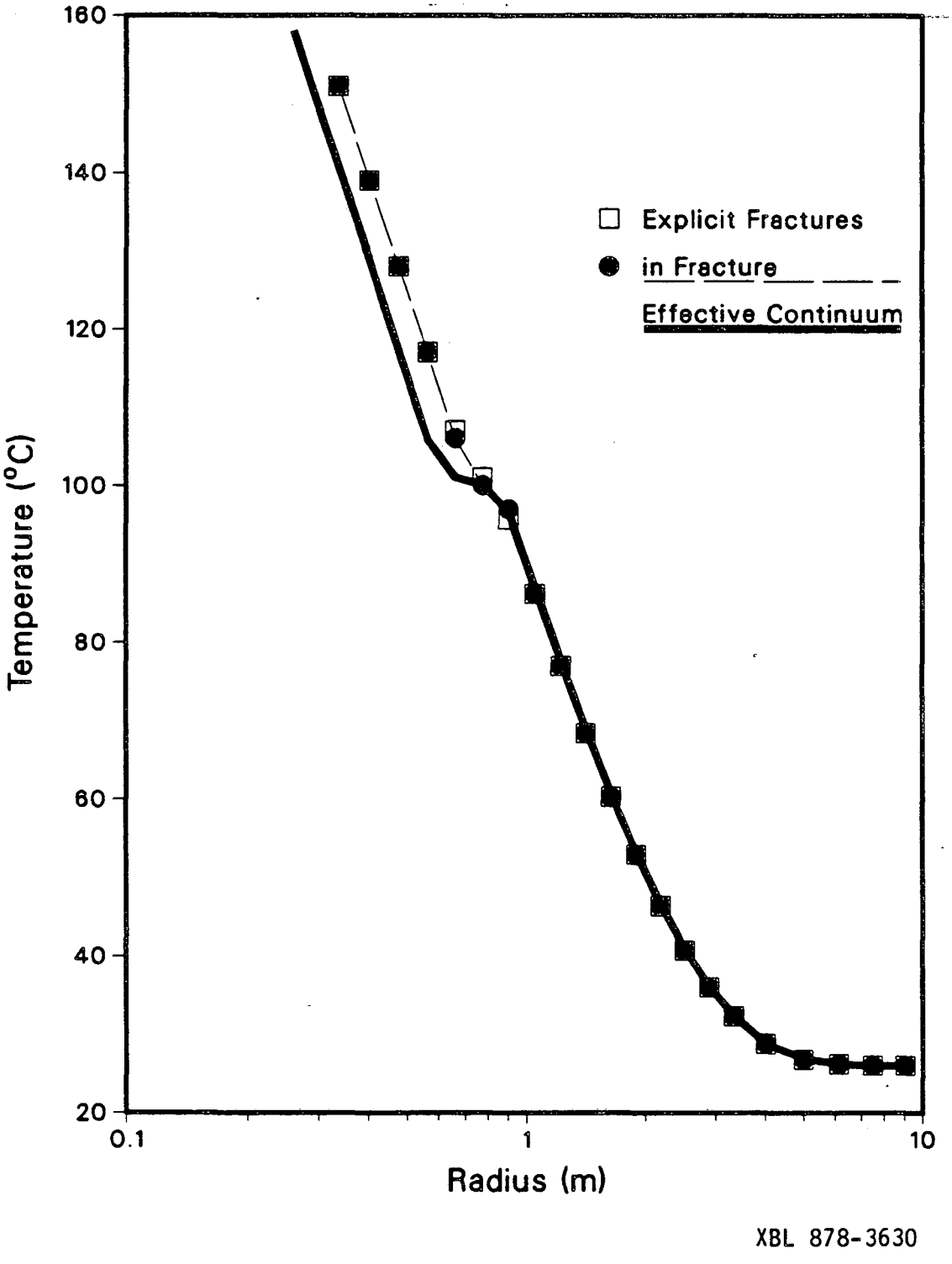

Figure 16. Temperature profiles at 36.5 days ("tight" matrix; backfilled emplacement conditions; the points labeled "explicit fractures" represent averages over the matrix domain).

LAWRENCE BERKELEY LABORATORY
TECHNICAL INFORMATION DEPARTMENT
1 CYCLOTRON ROAD
BERKELEY, CALIFORNIA 94720